A planar BPF for UWB communication systems with single/multiple interference rejection bands

Corresponding author: Abu Nasar Ghazali;
Email: anghazali@gmail.com;
abu.ghazalifet@kiit.ac.in

CAMBRIDGE
UNIVERSITY PRESS

Abu Nasar Ghazali[1] and Mohd Sazid[2]

[1]School of Electronics Engineering, Kalinga Institute of Industrial Technology, Deemed to be University, Bhubaneswar, India and [2]Department of Electronics and Communication Engineering, Delhi Technological University, Delhi, India

Abstract

The design and development of a microstrip-based planar ultra-wideband (UWB) bandpass filter (BPF) with single/multiple interference rejection capability is presented. The proposed BPF structure is developed based on the broadside coupled mechanism of microstrip/coplanar waveguide (CPW). The BPF has microstrips and short-circuited CPW capacitively coupled through the substrate. The basic frequency response generated from this geometry covers the necessary UWB spectrum (3.1–10.6 GHz) and possesses appreciable characteristics due to dual transmission zeros at either passband boundary. Multiple resonators are embedded in the basic BPF structure to develop passband notches to circumvent unnecessary interferences. A low-pass filter is later integrated into geometry to extend the upper stopband. The proposed structure is compact and covers an area of only 14×11.4 mm^2.

Introduction

The Federal Communications Commission (FCC) has mandated ultra-wideband (UWB) devices to use an emission mask (−75 mW/MHz) to minimize interference with other in-band wireless services [1]. However, because these in-band radio services, such as wireless local-area network (WLAN), C band, X band, etc., function as high-energy transmitters at their operating frequencies, they significantly interfere with the operation of UWB systems. Therefore, UWB-bandpass filter (BPF) with integrated band notch properties became necessary. Extensive research and development were conducted in designing and modeling UWB filters with interference-proof properties [2–17]. These BPFs developed triple passband notches using techniques such as, quarter-wavelength resonators of various shapes and designs [2–5], defected ground structures (DGS) [6–8], triple-mode step-loaded resonators [9–11], wave-cancellation technique [12, 13], and defected microstrip structures (DMS) [14]. Few other BPFs generated notches using combinations of the above described techniques [15–17]. Complementary split-ring resonator (CSRR), together with DGS plus folded multiple mode resonator (MMR), generated multiple notches in [15], whereas two MMR combined with CSRR produced triple notches in paper [16]. A dual-mode stepped impedance resonator (SIR) acting in combination with asymmetric coupling was the reason for the triple notch in the passband of [17]. However, these structures possessed several disadvantages such as absence of two transmission zeros (TZs) at the edges of UWB spectrum [2, 5–7, 9–11, 16, 17], tedious design because of soldered vias [9–13, 17], minimum design limitation of resonators [2, 3, 5–7, 10, 12, 16], and large physical/electrical circuit area [2–14]/[3–5, 9, 11].

Here, we propose a broadside coupled UWB filter with multiple passband TZs and an extended upper stopband. The broadside coupled technology of microstrip/coplanar waveguide (CPW) was adopted for the fundamental design of our BPF due to its inherent strong coupling and high selectivity, which provided good frequency characteristics [18, 19]. Our structure has two microstrip lines on the top plane and an short-circuited coplanar waveguide (SCCPW) in the ground plane of the common substrate. The response generated depicts a good passband response due to dual TZs at either spectrum edge. The basic BPF is then implanted with several resonators to produce multiple passband notches, and later, a low-pass filter (LPF) is embedded to extend the upper stopband. The proposed BPF is designed and optimized using the full-wave electromagnetic (EM) simulation software IE3D.

BPF analysis and design

The basic BPF structure consists of SCCPW and microstrips on either side of the substrate. We start the analysis by first modeling the SCCPW, followed by its optimized coupling with
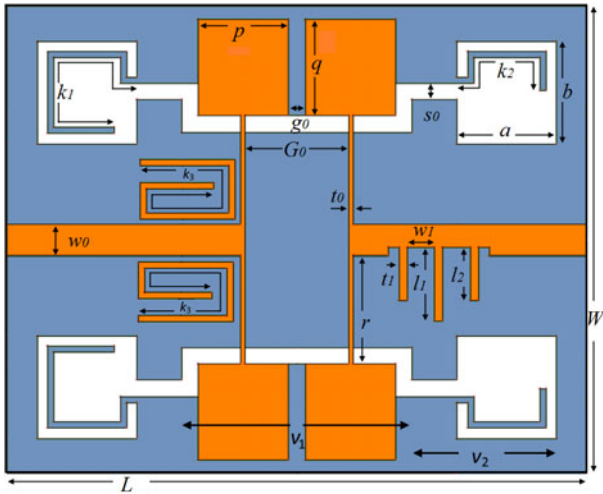
Figure 1. Geometrical representation of the proposed triple notched band BPF. Dark color is the conductor, whereas white shades are the slots. The optimized values are as follows: $w_0 = 0.76$ mm, $w_1 = 0.64$ mm, $g_0 = 0.4$ mm, $p = 2.18$ mm, $q = 2.35$ mm, $v_1 = 5.25$ mm, $v_2 = 3.5$ mm, $t_1 = 0.15$ mm, $l_1 = 1.78$ mm, $l_2 = 1.28$ mm, $k_1 = 5.62$ mm, $k_2 = 3.12$ mm, $k_3 =$ mm, $a = 2.4$ mm, $b = 2.4$ mm, $G_0 = 2.49$ mm, $L = 14$ mm, $W = 11.4$ mm.

the top plane. Figure 2(a) depicts the simplified topology of the SCCPW, whereas its transmission line equivalent is represented in Fig. 2(b). The central and end sections of the SCCPW have impedances and electrical lengths of Z_1, $2\theta_1$ and Z_2, θ_2. The input resistance Z_{input} at the left end looking into the right, for a general transmission line of electrical length θ, characteristic resistance Z_0 and terminated with load resistance Z_L, is given by [19]
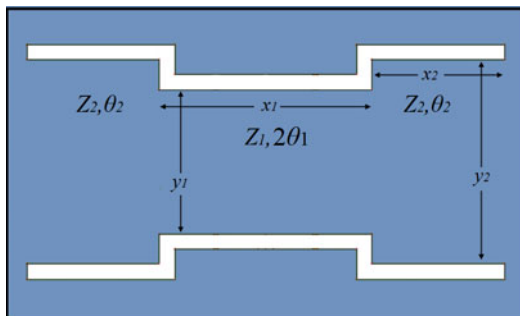
$$Z_{input} = Z_0 \left(\frac{Z_L + Z_0 j \tan \theta}{Z_0 + Z_L j \tan \theta} \right) \quad (1)$$

From Fig. 2, the input impedance Z_a, with characteristic resistance Z_2 and short-circuited load ($Z_L = 0$), can hence be written as

$$Z_a = Z_2 j \tan \theta_2 \quad (2)$$

Eventually, Z_{in} can be evaluated as

$$Z_{in} = Z_2 \left(\frac{Z_b + jZ_2 \tan \theta_2}{Z_2 + jZ_b \tan \theta_2} \right) \quad (3)$$

Placing the values of Z_b and Z_a in terms of Z_1, Z_2, ($R = Z_1/Z_2$) and including them in equation (3), we get

$$Z_{in} = jZ_2 \left(\frac{2(R \tan \theta_1 + \tan \theta_2)(R - \tan \theta_1 \tan \theta_2)}{\begin{array}{c} R \left(1 - tan^2\theta_1\right)\left(1 - tan^2\theta_2\right) \\ -2\left(1 + R^2\right) \tan \theta_1 \tan \theta_2 \end{array}} \right) \quad (4)$$

At resonance ($Z_{in} = 0$), equation (4) simplifies to

$$R \tan \theta_1 + \tan \theta_2 = 0 \quad (5)$$

and

$$R - \tan \theta_1 \tan \theta_2 = 0 \quad (6)$$

For the above structure, $\theta_1 \approx \theta_2 \approx \theta$, hence, equations (6) and (7) reduce to

$$R \tan \theta + \tan \theta = 0 \quad (7)$$

and

$$R - \tan^2 \theta = 0 \quad (8)$$

Solving the above equations using the analytical method gives three resonant frequencies:

$$\theta \left(f_\alpha \right) = \tan^{-1} \left(\sqrt{R} \right) \quad (9)$$

$$\theta \left(f_\beta \right) = \frac{\pi}{2} \quad (10)$$

$$\theta \left(f_\gamma \right) = \pi - \tan^{-1} \left(\sqrt{R} \right) \quad (11)$$

The central section of SCCPW has, $x_1 = 5.25$ mm, $y_1 = 5.55$ mm, $s_0 = 0.4$ mm, for which $Z_1 = Z_{0(CPW1)} = 38.9$ Ω and $\theta_1 = 39.3°$. Similarly, the wider end sections have $x_2 = 2.48$ mm, $y_2 = 6.86$ mm and $s_0 = 0.4$ mm corresponding to $Z_2 = Z_{0(CPW2)} = 37.83$ Ω and $\theta_2 = 36.31°$. Therefore, $R = Z_1/Z_2 \approx 1$.

Post the design of SCCPW, its optimized coupling with the microstrip lines on the top plane is considered using the knowledge that maximum coupling of broadside transition of CPW/microstrip occurs for [18],

$$Z_{0(microstrip)} = 2Z_{0(CPW1)} \quad (12)$$

For our filter under consideration, with $t_0 = 0.15$ mm, $Z_{0(microstrip)} = 81.4$ Ω is obtained, and as calculated above,

(a)
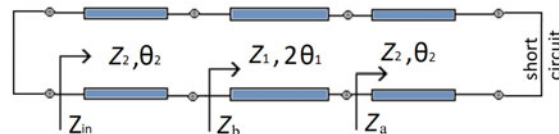
(b)

Figure 2. (a) Topology of the MMR for the proposed BPF. Wide arm of characteristic impedance and electrical length Z_1, θ_1 respectively, while the narrow arm has characteristic impedance and electrical length Z_2, θ_2 respectively. (b) Equivalent transmission line model of the MMR.
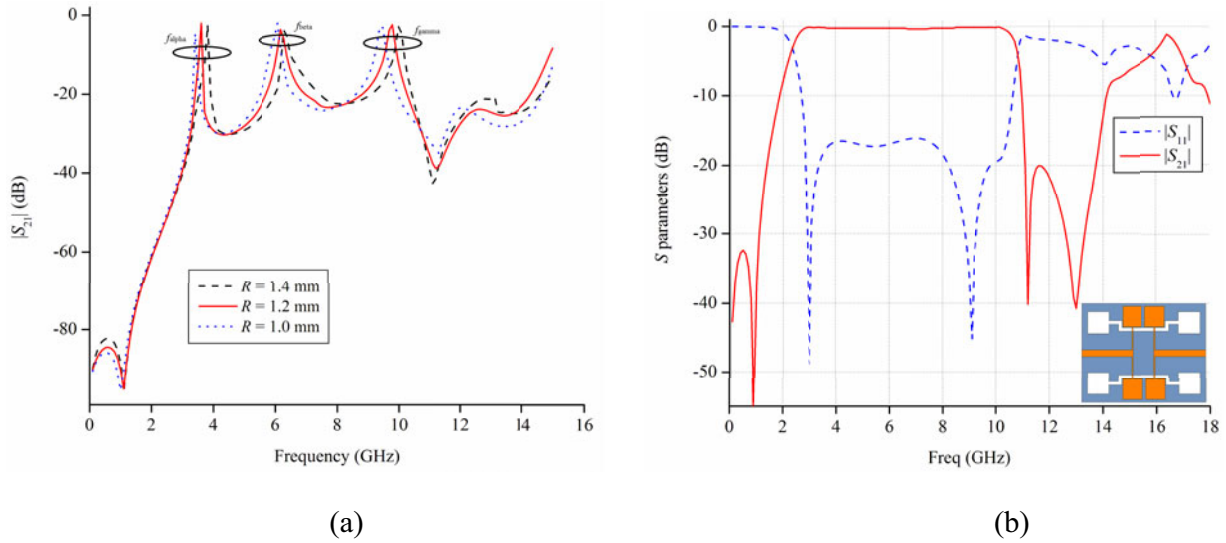
Figure 3. (a) Frequency response of the basic BPF for weak coupling. (b) Optimized frequency response of the broadside coupled UWB-BPF.

$Z_{0(CPW1)} = Z_1 = 38.9\ \Omega$, i.e., equation (12) is balanced. Later, in CPW2, the slot ends are modified to square-shaped DGS to adjust the 3-dB cutoff bandwidth of the filter. Figure 3(a) provides us with the weak coupling response for various values of R and the optimized simulated response of the basic broadside coupled BPF is provided in Fig. 3(b). It can be observed that the passband of BPF extends from 2.35 to 10.78 GHz with return/insertion loss better than 17/0.38 dB. The BPF depicts steep selectivity of >47 and >128 dB/GHz respectively, at lower and upper passband edges due to TZs at 0.95 and 11.2 GHz. The third TZ at 13 GHz extends the stopband till 14 GHz.

Notched band implementation and upper stopband extension

Due to the emission mask (-75 mW/MHz) imposed by FCC on UWB systems, they seldom become the source of interference. However, other wireless services like WLAN, C band, X band, etc., present within the UWB passband, are high-power radio-frequency emitters, cause interference [1]. UWB-BPFs are often embedded with bandstop filters (BSFs) to eliminate such interfering threats. These BSFs could be in the form of resonators [2–5, 9–13], DGS [6–8], DMS [14], appended to or coupled with the basic BPF geometry. Here, we inculcate the bandstop filtering characteristics using only resonators, a few of which are embedded in the ground and two independent ones coupled to the top (Fig. 1). These resonators are varied in length to tune their notch frequency and placed at our point of interest within the passband. The resonator lengths are related to their corresponding notch frequency positions through the following equations:

$$f\,(@5.2\ \text{GHz}) \approx c/\left\{2l_{k1}\sqrt{\varepsilon_{\text{reff}}}\right\} \qquad (13)$$

$$f\,(@6.5\ \text{GHz}) \approx c/\left\{2l_{\text{FSRR}}\sqrt{\varepsilon_{\text{reff}}}\right\} \qquad (14)$$

$$f\,(@7.9\ \text{GHz}) \approx c/\left\{2l_{k2}\sqrt{\varepsilon_{\text{reff}}}\right\} \qquad (15)$$

where c is the velocity of light and $\varepsilon_{\text{reff}} = 6.08$. It is observed that at their frequency of operation, the resonators are approximately a quarter of their guided wavelength. Figure 4 below depicts the depth of tuning of the single/multiple notches within the UWB passband for variable length of each resonator, respectively. This above property helps eradicate unwanted interferences at any operating frequency within the UWB spectrum.

The basic BPF (Fig. 3) depicts good frequency characteristics in terms of its passband and lower stopband. However, the upper stopband needs some attending to. In that respect, LPF, in the form of multiple stubs, is appended to the output feeding line [19, 20]. These stubs develop TZ at 14.7 GHz in the stopband to reduce the attenuation below -17 dB and extend the stopband to 18 GHz. Figure 5 below depicts the comparative frequency response of single/multiple notched BPFs with and without embedded LPF. It can be observed that these BPFs have upper stopband attenuated below -17 dB and extended till 18 GHz.

The current distribution across the BPF structure is portrayed in Fig. 6, which depicts that at their respective frequencies of operation (5.2, 6.5, and 7.9 GHz), the resonators have the highest current concentration, whereas at 14.7 GHz, the current density is maximum in the LPF. The current density concentration on a particular component of the BPF at that frequency depicts its activeness compared to other components. An approximate equivalent lumped element circuit model of the proposed BPF is constructed (Fig. 7a), and its response is observed against the full-wave EM simulation data in Fig. 7(b). The input feeding line is represented by L_6, whereas the parallel combination of L_7 and C_{11} represents the output feeding line embedded with the LPF. The parallel combination of L_1 and C_1 represents the stubs attached to input/output feeding lines, whereas their separation is depicted by the gap capacitance C_0. The tank circuit consisting of L_4, C_4, and C_8 portrays the SCCPW-based ground plane in which variable length resonators (described by parallel circuits L_2, C_2 and L_3, C_3) are coupled through capacitances C_6 and C_7. The FSRRs are depicted by the combination of L_5, C_5, and C_9 coupled to the BPF structure through C_{10}.
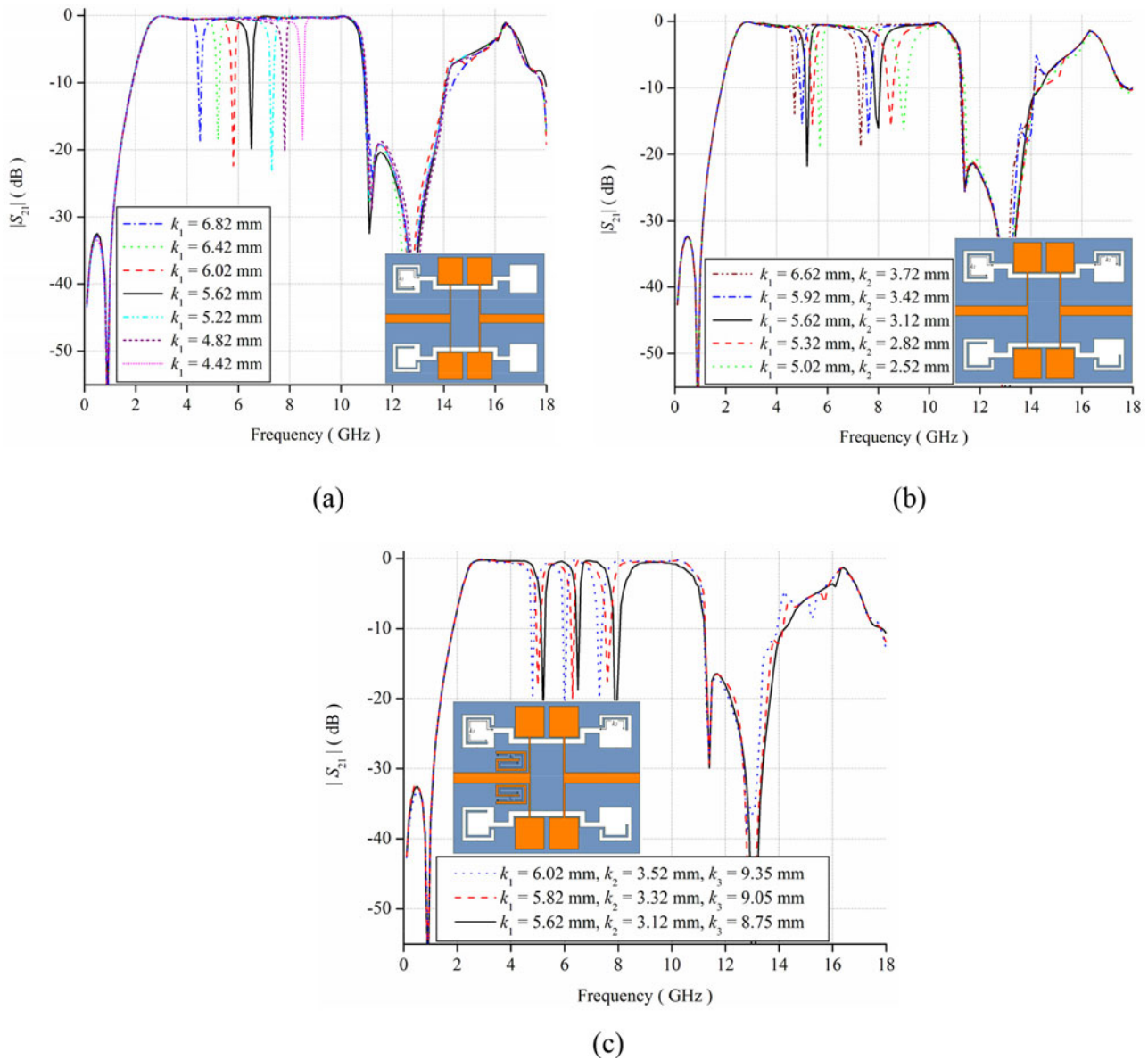
Figure 4. Dynamic positions of (a) single notches for variable values of k_1, (b) dual notches for variable values of k_1 and k_2, (c) triple notches for variable values of k_1, k_2, and k_3.

The equivalent circuit model of the proposed UWB filter is based on paper [21]. The location of the notches is evaluated from paper [21], as

$$f_{\text{lower TZ}} = 1/\{2\pi\sqrt{(L_1C_1 + L_1C_0)}\} \qquad (16)$$

for $L_1 = 4.3$ nH, $C_1 = 5.46$ pF, and $C_0 = 0.022$ pF, we get $f = 0.95$ GHz.

$$f_{(@ 5.2 \text{ GHz})} = 1/\{2\pi\sqrt{(L_2C_2 + L_2C_6)}\} \qquad (17)$$

for $L_2 = 1.36$ nH, $C_2 = 0.3275$ pF, and $C_6 = 0.355$ pF, we get $f = 5.22$ GHz.

$$f_{(@ 6.5 \text{ GHz})} = 1/\{2\pi\sqrt{(L_5C_5 + L_5C_9)}\} \qquad (18)$$

for $L_5 = 0.721$ nH, $C_5 = 0.21$ pF, and $C_9 = 0.6145$ pF, we get $f = 6.55$ GHz.

$$f_{(@ 7.9 \text{ GHz})} = 1/\{2\pi\sqrt{(L_3C_3 + L_3C_7)}\} \qquad (19)$$

for $L_3 = 1.312$ nH, $C_3 = 0.1875$ pF, and $C_7 = 0.1224$ pF, we get $f = 7.86$ GHz.

It can be observed from above that the values obtained analytically are quite close to that obtained from full-wave EM simulation and circuit simulation. The values of the remaining parameters are fine-tuned using the software. The optimized parametric values of the components are as follows:

$C_0 = 0.022$ pF, $C_1 = 5.46$ pF, $C_2 = 0.3275$ pF, $C_3 = 0.1875$ pF, $C_4 = 0.63$ pF, $C_5 = 0.21$ pF, $C_6 = 0.355$ pF, $C_7 = 0.1224$ pF, $C_8 = 0.508$ pF, $C_9 = 0.6145$ pF, $C_{10} = 0.25$ pF, $C_{11} = 0.01$ pF,
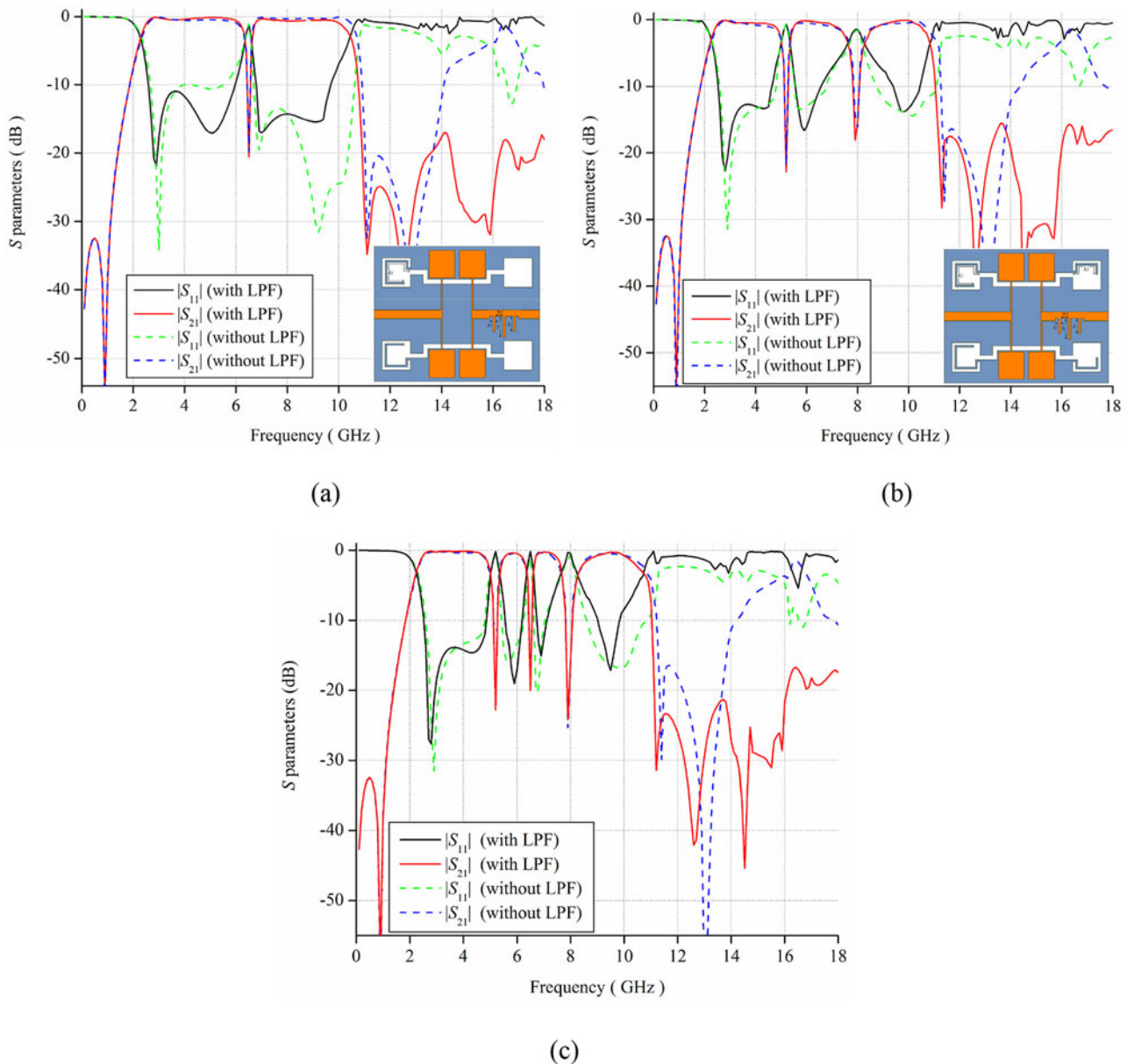
Figure 5. Comparative frequency responses of the single, double, and triple band-notched UWB filter with and without LPF.

$L_1 = 4.3$ nH, $L_2 = 1.36$ nH, $L_3 = 1.312$ nH, $L_4 = 1.496$ nH, $L_5 = 0.721$ nH, $L_6 = 0.274$ nH. $L_7 = 0.614$ nH.

Fabrication, measurement, and results

The proposed structure is fabricated using the photolithographic effect (chemical etching) and put up for testing using Agilent Vector Network Analyzer N5230A. The data derived from the test is observed and analyzed against simulation results in Fig. 8. It is observed from the measured result that the 3-dB passband is from 2.4 to 10.62 GHz, with three notches at 5.11, 6.4, and 8 GHz having 3-dB fractional bandwidth (FBW) of 3.2%, 2.6%, and 4.4% respectively and attenuation of at least −20 dB. The insertion/return loss within the passband is better than 0.76/12.8 dB before the first notch, 0.63/24 dB between the first and second notch, 0.68/11 dB

between the second and third notch, and 0.83/13 dB after the third notch. The passband group delay variation is between 0.22 and 0.62 ns, except at the triple notches. The upper stopband is 18 GHz wide with attenuation greater than 19 dB. The misalignment between measured and simulated data be attributed human error in fabrication/measurement, finite active circuit area of the BPF, and reflections off connectors. An exhaustive comparative study of our proposed triple notched-BPF with other similar BPFs available in the literature is presented in Table 1. The table portrays that papers [2, 8, 10, 12–15] do not possess the necessary UWB passband bandwidth. Papers [6, 7, 9–11, 17] lack the presence of TZs at both passband edges, whereas papers [2, 4, 5, 16] possess TZ only at one passband edge. Our proposed structure is physically smaller than all except paper [8], whereas it is electrically smaller (at the central UWB frequency) than papers [3, 4, 6, 7, 11, 14–16]
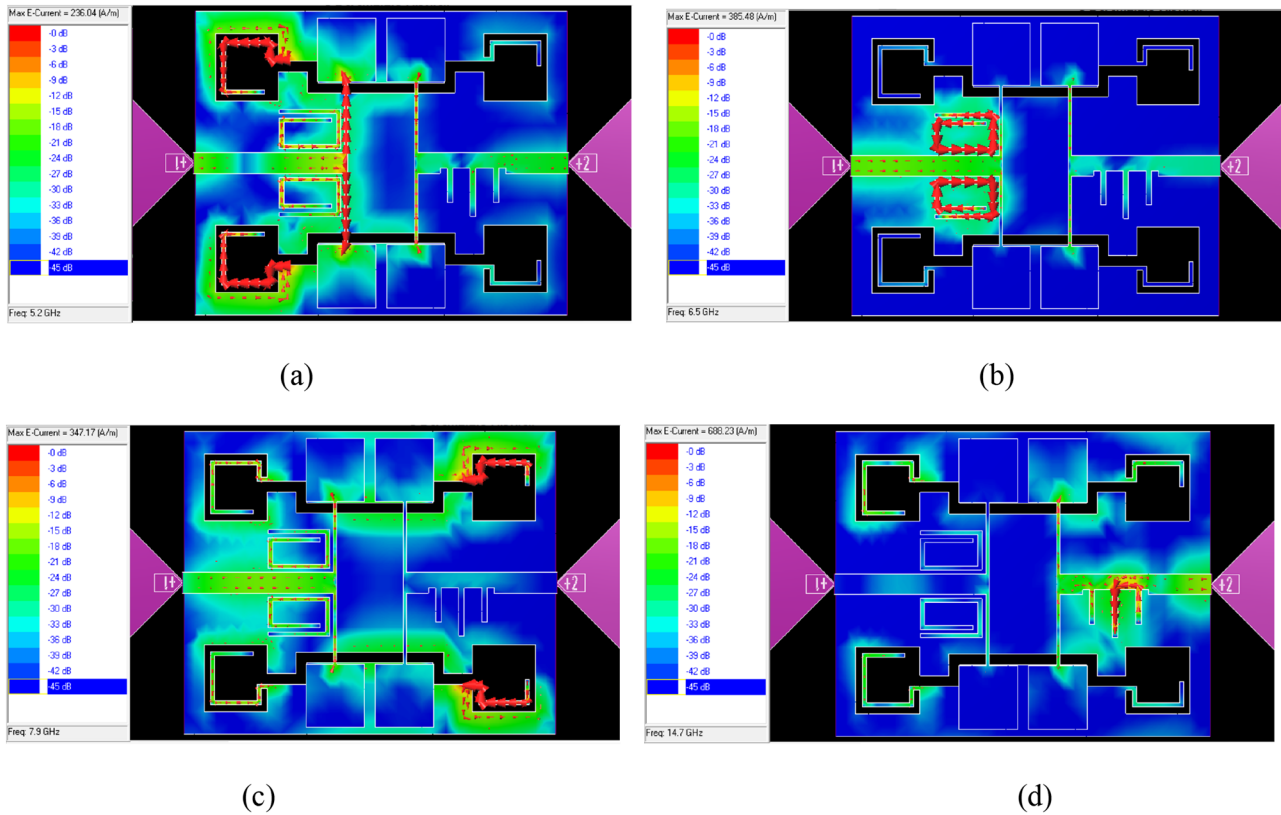
Figure 6. Current distribution in the proposed triple-notched BPF at their respective frequencies of (a) 5.2, (b) 6.5, (c) 7.9, and (d) 14.7 GHz.
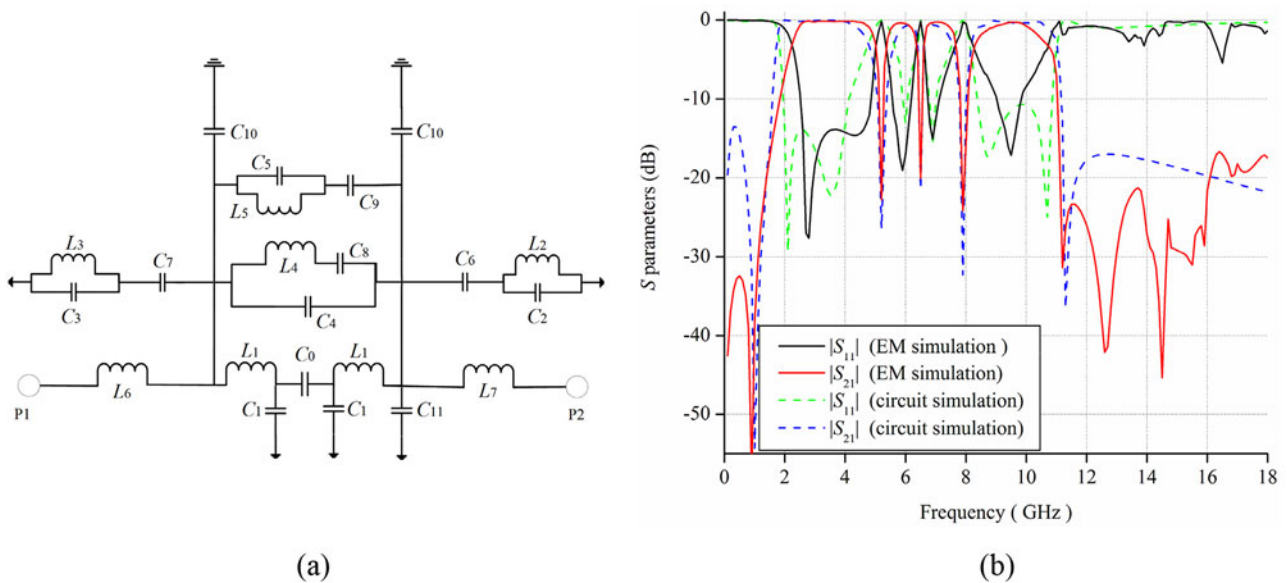

Figure 7. (a) Approximate equivalent circuit model of the proposed triple notched band BPF. (b) Comparative frequency characteristics for full-wave EM and circuit simulation.

and comparable to the rest. Also, our BPF has simple geometrical construction, unlike papers [9–13], which possess vias, and papers [2, 3, 10, 12, 17], whose design are limited by fabrication due to minimal dimension constrains. The implementation of vias in such delicate microstrips needs expertise in drilling and soldering, for any unnecessary soldering may bring about impedance

mismatch, thereby affecting the frequency characteristics. Also, improper drilling could lead to the destruction of the BPF. With all the information provided above, it can be concluded that the proposed triple-notched UWB-BPF is simple to design and implement, meets all necessary frequency requirements, hence, better than its contemporaries.
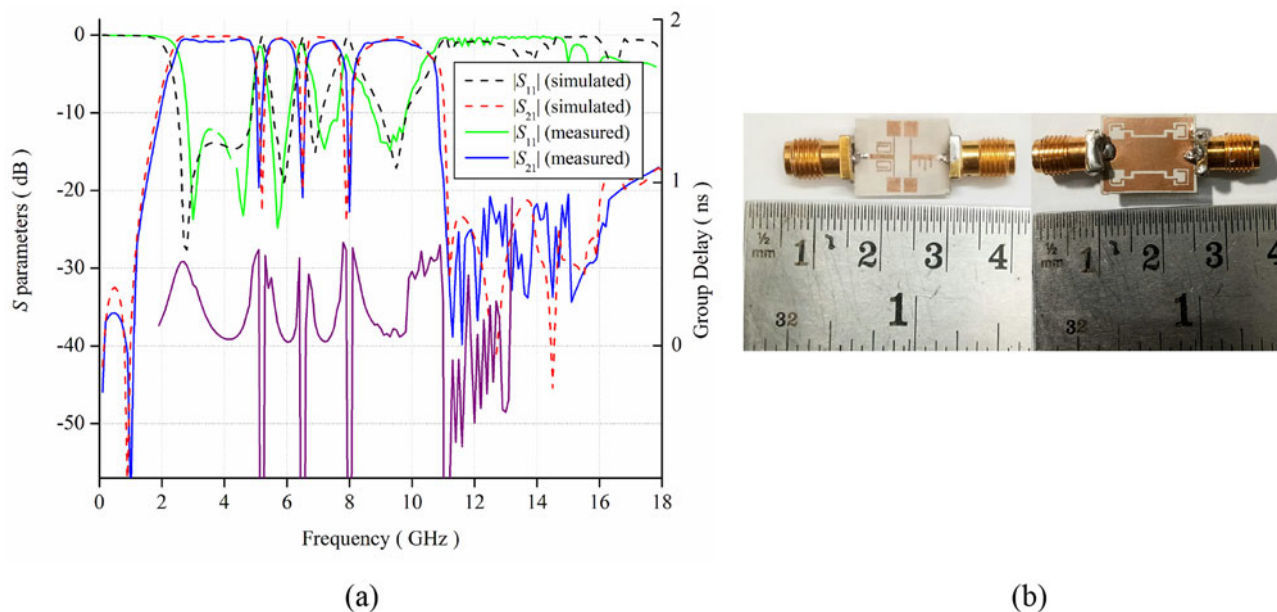
Figure 8. (a) Comparative measured and simulated frequency characteristics. (b) Fabricated prototype.

Table 1. Comparison of present triple notched-BPF with recently known other triple-notched structures in literature

Ref.	Passband (GHz)	TZs at either passband edges	Notches (GHz)/Attenuation (dB)	Stopband (GHz)/Attenuation (dB)	SF ($\Delta f_{3dB}/\Delta f_{30dB}$)	Electrical size ($\lambda_g \times \lambda_g$)
[2]	4.3–10.2	×, √	5.9, 8, 9/>18	15/>14	<0.6	>0.7 × 0.2
[3]	3.1–10.6	√, √	3.6, 5.3, 8.4/> 16	17/>18	0.975	>1.2 × 0.7
[4]	3.1–10.62	×, √	5.2, 5.8, 7.9/>16	16/>15	<0.75	>1.2 × 0.75
[5]	2.86–10.72	√, ×	6, 6.53, 8.35/>15	16/>20	<0.85	0.81 × 0.71
[6]	2.7–10.6	×, ×	5.2, 6.1, 8.15/ > 18	18/>26	<0.75	1.8 × 0.78
[7]	2.1–11.5	×, ×	5.5, 6.2, 8.2/>15	18/>23	<0.75	1.8 × 0.78
[8]	3.25–10.73	√, √	5.6, 6.42, 8.03/>19	17/>16	<0.85	1.04 × 0.66
[9]	2.8–11	×, ×	5.2, 5.85, 8/>10	20/>10	<0.7	1 × 0.66
[10]	3–10.3	×, ×	5.2, 5.8, 6.8/>15	30/>15	<0.65	0.67 × 0.43
[11]	2.8–10.6	×, ×	3.3, 5.1, 8.3/>12	11/>10	<0.55	>1.67 × 0.67
[12]	3.3–10.7	√, √	4.4, 5.5, 7.64/ > 14	20/>20	0.89	>1 × 0.65
[13]	3.5–10.85	√, √	5.4, 5.8, 8.3/>18	15/>11	<0.8	>1.15 × 0.5
[14]	3–10.2	√, √	5.2, 5.8, 8/>15	17/>12	<0.9	>1.22 × 0.8
[15]	2.6–8.3	√, √	4.8, 5.2, 6.4>11	11/>19	<0.75	1.22 × 0.53
[16]	3.2–12	√, ×	4.1, 6.6, 9/>13	14/>10	<0.65	>1.24 × 0.32
[17]	3.1–10.6	×, ×	5.85, 7.12, 8.13 > 21	17/>17	<0.6	>0.93 × 0.37
This work	2.9–10.75	√, √	5.11, 6.4, 8>19	18/>17	0.82	0.95 × 0.78

Conclusion

An UWB-BPF with single/multiple band notch characteristics is proposed and implemented. Developed on the broadside coupled mechanism of microstrip/CPW, capacitively coupled to each other through the substrate, this geometry generates appreciable frequency characteristics with multiple TZs. Later, several resonators are embedded in the basic BPF structure to develop pass-band notches to cut out unnecessary interferences. Finally, a LPF is appended to the geometry to widen the upper stopband and improve isolation. The proposed structure is compact and possesses an edge over its contemporaries, because of which it is an ideal candidate for implementation in UWB communication systems.

Competing interests. The authors declare that they have no known competing financial interests or personal relationships that could have appeared to

influence the work reported in this paper. The authors declare the following financial interests/personal relationships which may be considered as potential competing interests.

References

1. **Federal Communications Commission (FCC)** (2002) Revision of part 15 of the commission's rules regarding ultra-wideband transmission systems. Report and Order in ET Docket, 98–153.

2. **Shi XM, Xi XL, Zhao YC and Yang HL** (2015) A novel compact ultra-wideband (UWB) bandpass filter with triple-notched bands. *Journal of Electromagnetic Waves and Applications* **29**(9), 1174–1180.

3. **Kumar S, Gupta RD and Parihar MS** (2016) Multiple band notched filter using C-Shaped and E-Shaped resonator for UWB applications. *IEEE Microwave and Wireless Components Letters* **26**, 340–342.

4. **Taibi A, Trabelsi M and Saadi A** (2021) Efficient design approach of triple notched UWB filter. *AEU - International Journal of Electronics and Communications* **131**, 153619.

5. **Chakraborty P, Shome PP, Panda JR and Deb A** (2022) Highly selective UWB bandpass filter with multi-notch characteristics using comb shaped resonator. *Progress In Electromagnetics Research M* **108**, 89–101.

6. **Ghazali AN and Pal S** (2015) Planar UWB filter with multiple notched band and stopband with improved rejection level. *Frequenz* **69**, 207–218.

7. **Ghazali AN and Pal S** (2013) Microstrip based UWB filter with controllable multiple notches and extended upper stopband. In *International Conference on Emerging Trends in Communication, Control, Signal Processing and Computing Applications (C2SPCA)*. Bangalore: IEEE, 1–5.

8. **Sazid M and Raghava NS** (2021) Planar UWB-bandpass filter with multiple passband transmission zeros. *AEU - International Journal of Electronics and Communications* **134**, 153711.

9. **Wei F, Li WT, Shi XW and Huang QL** (2012) Compact UWB bandpass filter with triple-notched bands using triple-mode stepped impedance resonator. *IEEE Microwave and Wireless Components Letters* **22**, 512–514.

10. **Peng H, Zhao J and Wang B** (2014) Compact microstrip UWB bandpass filter with triple-notched bands and wide upper stopband. *Progress In Electromagnetics Research* **144**, 185–191.

11. **Basit A, Khattak M and Hasan M** (2020) Design and analysis of a microstrip planar UWB bandpass filter with triple notch bands for WiMAX, WLAN, and X-Band satellite communication systems. *Progress in Electromagnetics Research M* **93**, 155–164.

12. **Kamma A, Das R, Bhatt D and Mukherjee J** (2017) Multi-mode resonators based triple band notch UWB filter. *IEEE Microwave and Wireless Components Letters* **27**, 120–122.

13. **Gholipoor M, Honarvar MA and Virdee BS** (2016) UWB bandpass filters with triple notched band characteristics implemented using wave cancellation technique. *Microwave and Optical Technology Letters* **58**, 1875–1879.

14. **Wang J, Zhao J and Li JL** (2014) Compact UWB bandpass filter with triple notched bands using parallel U shaped defected microstrip structure. *Electronics Letters* **50**, 89–91.

15. **Chiang C-T, Xu J-C and Liu J-C** (2014) Compact ultrawideband bandpass filter with triple notched-bands and sharp transmission zeros based on CSRR, DGS, and FMRR configurations. *Microwave and Optical Technology Letters* **56**, 2324–2330.

16. **Borazjani O, Nosrati M and Daneshmand M** (2014) A novel triple notch-bands ultra wide-band band-pass filters using parallel multi-mode resonators and CSRRs. *International Journal of RF and Microwave Computer-Aided Engineering* **24**, 375–381.

17. **Liu JQ, Song KJ and Fan Y** (2012) UWB BPF with triple notched bands using novel dual-mode SIR and asymmetrical coupling structure. *Journal of Electromagnetic Waves and Applications* **26**(16), 2112–2120.

18. **Baik JW, Lee TH and Kim YS** (2007) UWB bandpass filter using microstrip-to-CPW transition with broadband balun. *IEEE Microwave and Wireless Components Letters* **17**, 846–848.

19. **Zhu L, Sun S and Li R** (2012) Microwave Bandpass Filters for Wideband Communications. New York: John Wiley & Sons.

20. **Li R and Zhu L** (2007) Ultra-wideband microstrip-slotline bandpass filter with enhanced rejection skirts and widened upper stopband. *Electronics Letters* **43**(24), 960–961.

21. **Lin WJ, Li JY, Chen LS, Lin DB and Houng MP** (2010) Investigation in open circuited metal lines embedded in defected ground structure and its applications to UWB. *IEEE Microwave and Wireless Components Letters* **20**, 148–150.

Abu Nasar Ghazali received his B.Tech degree in Electronics & Communication Engineering (ECE) from SRM University, Chennai, in 2008 and M.E degree in Microwave Engineering from Birla Institute of Technology (BIT) Mesra, in 2010 where he was a GATE scholar. He completed his doctorate in 2014 from BIT Mesra. He worked as an Assistant Professor (I) in the Dept. of ECE at the BIT Mesra, Patna campus. Currently he is an Associate Professor in the School of Electronics Engineering, at the Kalinga Institute of Industrial Technology (KiiT), Bhubaneswar, India. He is an Associate member, The Institution of Engineers (IEI), India. He has published quite a few papers in SCI/SCOPUS indexed journals and conferences. His main research interests include UWB filters, microstrip filters, and passive microwave circuit components.

Mohd Sazid received his B.Tech degree in ECE from Uttar Pradesh Technical University in 2011 and M.E degree in Wireless Communication Engineering from BIT Mesra in 2015 where he was a GATE scholar. He is currently working as an Assistant Professor in the Department of ECE at the Noida Institute of Engineering and Technology. He has published several papers in SCI indexed journals. His main research interests include UWB filters and microstrip-based passive circuit components.